Supplementary materials

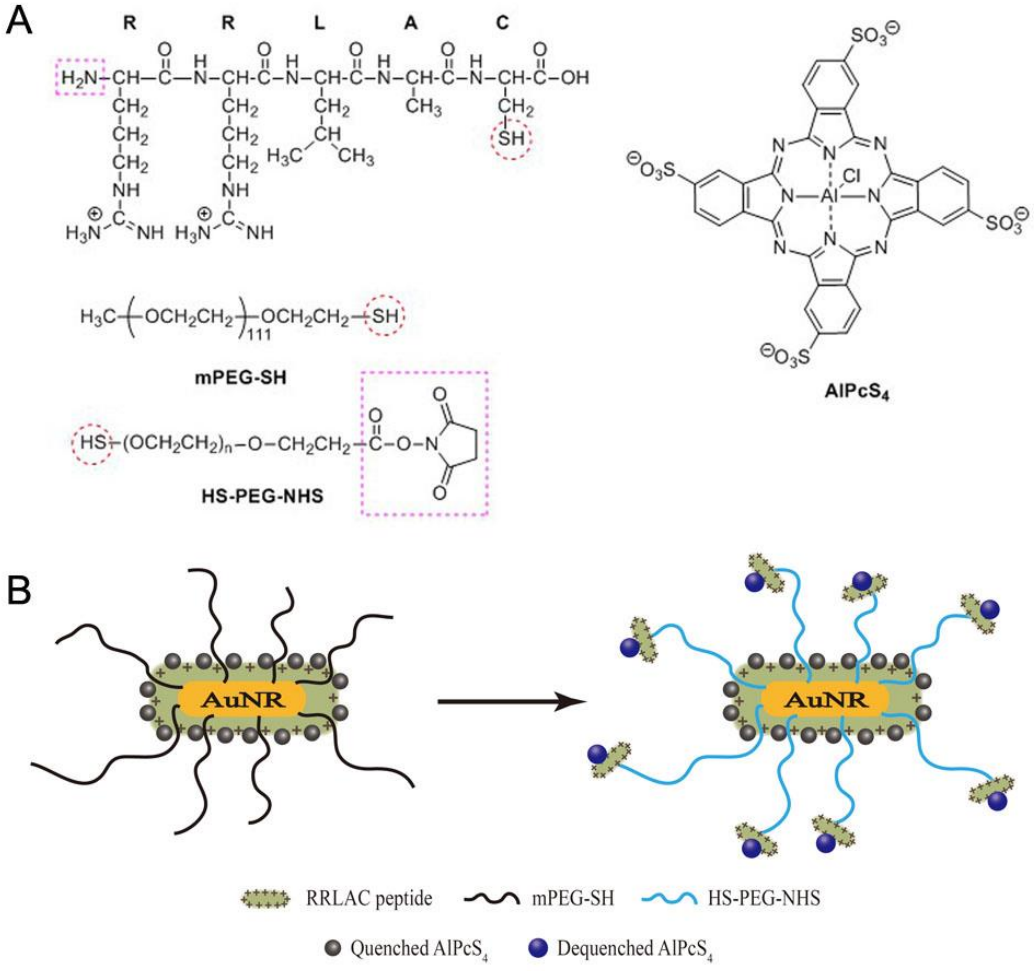

Figure S1: Chemical structure of RRLAC peptide, mPEG-SH, HS-PEG-NHS, and $AlPcS_4$ (A) and schematic diagram of the AuNR-$AlPcS_4$ complex AuNR-$AlPcS_4$ carriers based on mPEG-SH and HS-PEG-NHS (B).

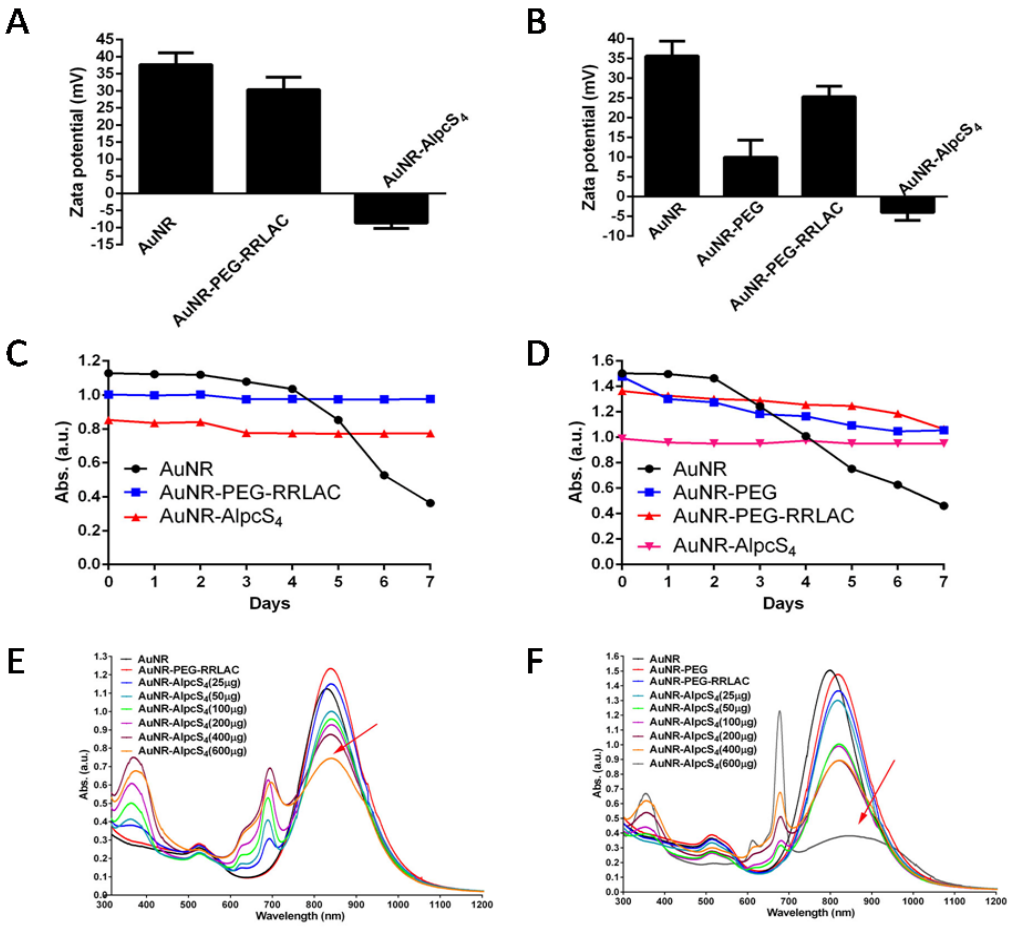

Figure S2: Difference of AuNR-AlPcS$_4$ carriers based on HS-PEG-NHS in one-step synthesis method and mPEG-SH in two-step synthesis method. Surface zeta potential of compounds based on HS-PEG-NHS (A) and mPEG-SH (B) in synthesis route; the photostability of compounds based on HS-PEG-NHS (C) and mPEG-SH (D) in synthesis route; and the UV-vis absorption spectra of compounds based on HS-PEG-NHS (E) and mPEG-SH (F) in synthesis route.

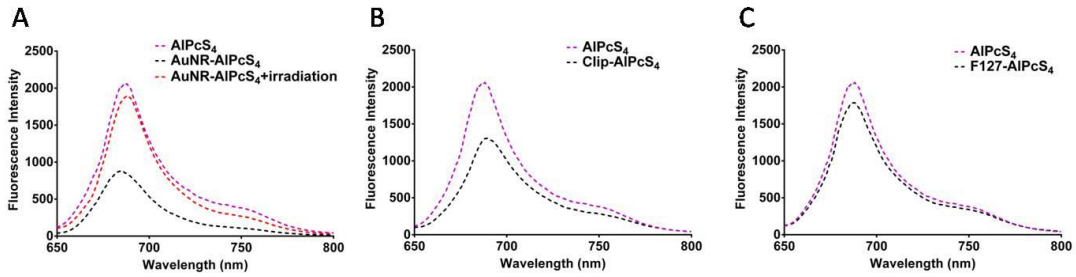

Figure S3: The fluorescence intensity of AuNR-AlPcS$_4$ with or without irradiation (A), Clip-AlPcS$_4$ (B) and F127-AlPcS$_4$ (C).

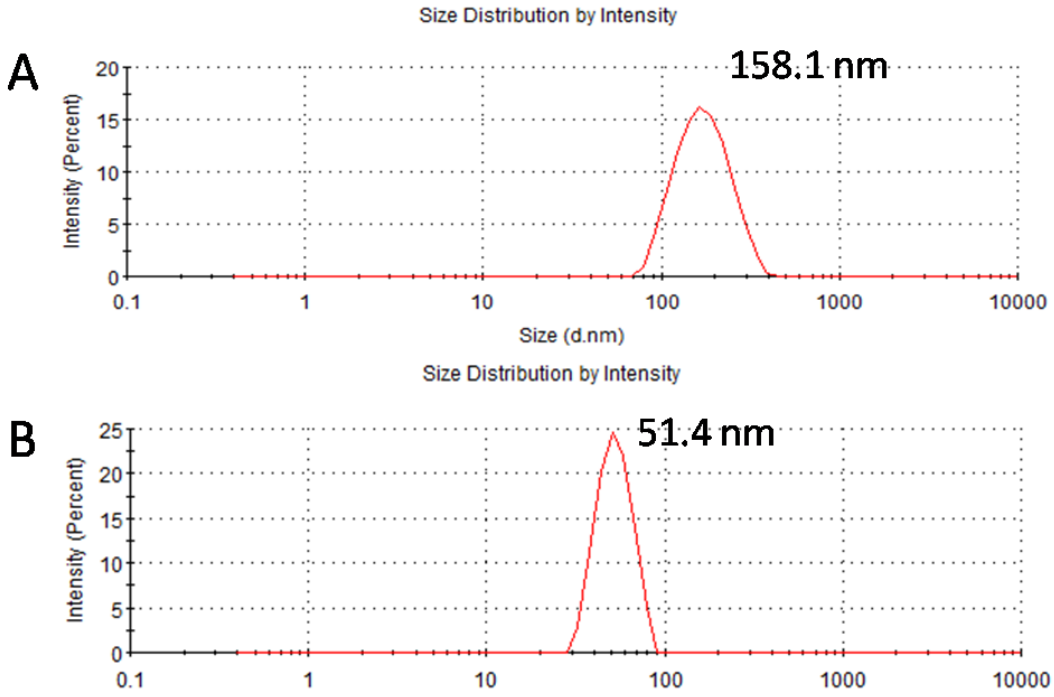

Figure S4: Dynamic light scattering of cationic liposome (A) and F127 nano-micelle(B).

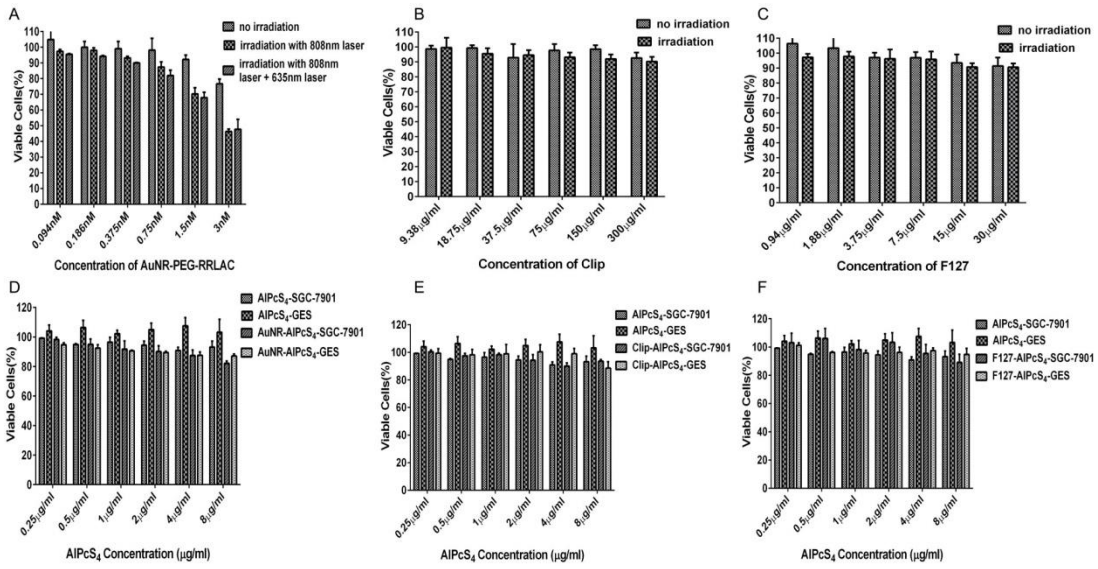

Figure S5: The dark cytotoxicity and photo-cytotoxicity of AuNR-PEG-RRLAC (A), Clip (B) and F127 (C) on SGC-7901 cells and the comparison of cytotoxic activity induced by AuNR-AlPcS$_4$ (D), Clip-AlPcS$_4$ (E) and F127-AlPcS$_4$ (F) between gastric cancer cell SGC-7901 and human immortalized fetal gastric epithelial cell GES evaluated by CCK-8 assay.

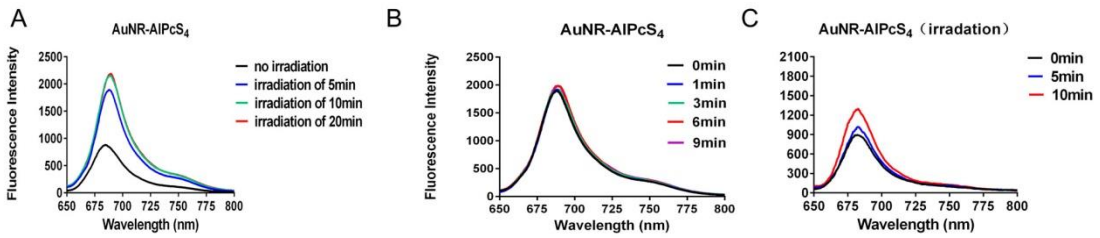

Figure S6: Fluorescence recovery time of $AlPcS_4$ releasing from AuNR surface. Fluorescence intensity of AuNR-$AlPcS_4$ irradiated by 808nm laser light at different durations (A). Fluorescence intensity changes with time after irradiation (B). Fluorescence intensity changes of AuNR-$AlPcS_4$ in SGC-7901 cells with time after being irradiated with 808nm laser light (C).

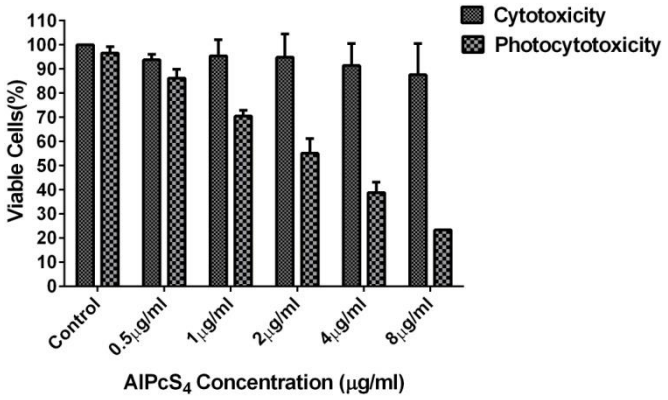

Figure S7: Anti-growth effect of F127-$AlPcS_4$ for 24hours (treatment time) on gastric cancer cells with or without irradiation. SGC-7901 cells were treated with 0.5-8μg/ml F127-$AlPcS_4$ for 24hours, irradiated with or without 635nm laser light, incubated with a fresh complete medium for another 24hours and then treated with a CCK-8 reagent for cell viability assay.

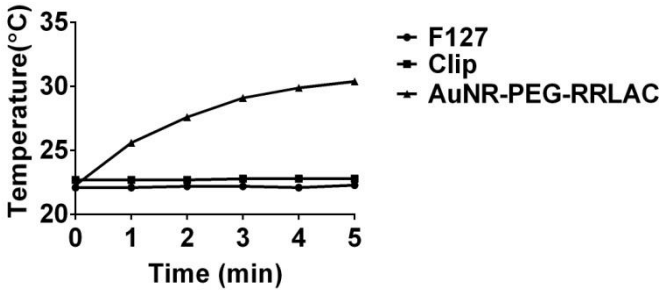

Figure S8: The temperature variation of AuNR-PEG-RRLAC, Clip and F127 after laser irradiation.

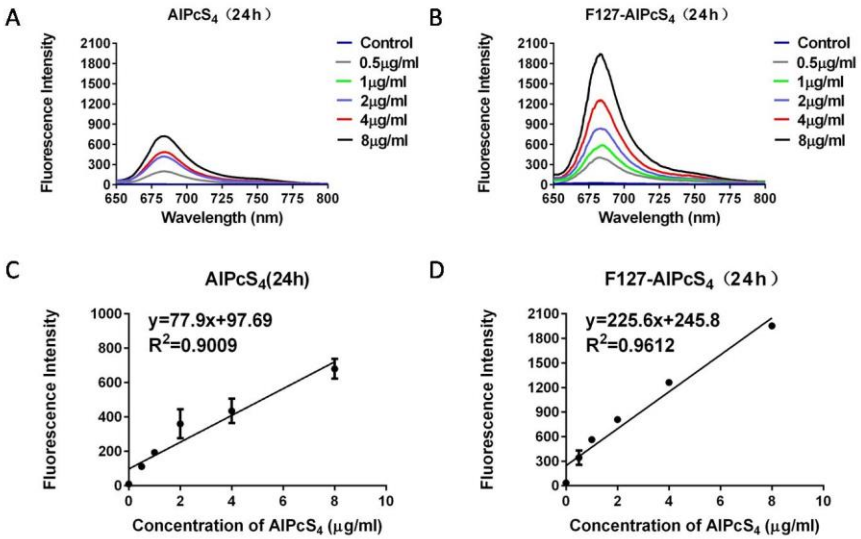

Figure S9: Evaluation of $AlPcS_4$ delivery efficiency of F127-$AlPcS_4$ carrier in SGC-7901 cells for 24hours (treatment time). Fluorescence intensity of $AlPcS_4$ and F127-$AlPcS_4$ in SGC-7901 cells after being treated with $AlPcS_4$ (A) and F127-$AlPcS_4$ (B) for 24hours at 0.5-8μg/ml, respectively. The correlation between concentration and fluorescence intensity of $AlPcS_4$ (C) and F127-$AlPcS_4$ (D) in SGC-7901 cells after being treated with $AlPcS_4$ and F127-$AlpcS_4$ for 24hours at 0.5-8μg/ml, respectively.

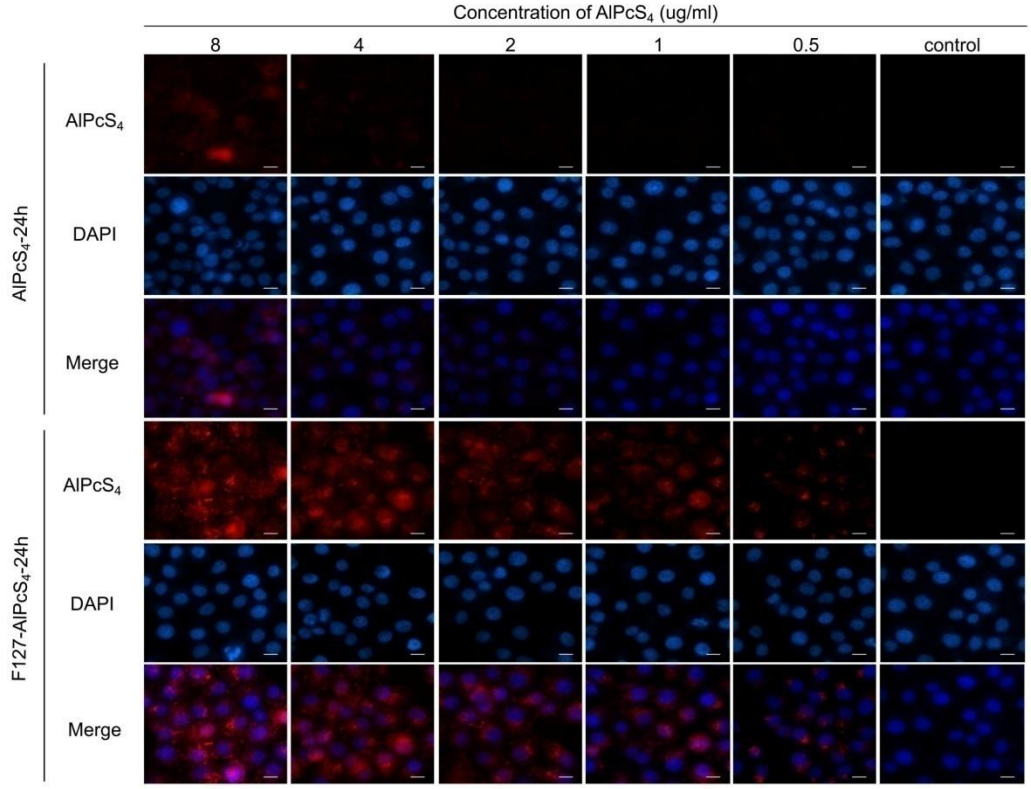

Figure S10: Fluorescence imaging of $AlPcS_4$ and F127-$AlPcS_4$ carrier delivery carrier in SGC-7901 cells for 24hours (treatment time). The SGC-7901 cells were treated with $AlPcS_4$ and F127-$AlPcS_4$ at 0.5-8μg concentrations for 24hours, and then stained with DAPI (nuclear staining) and imaged. The Bar=20μm.

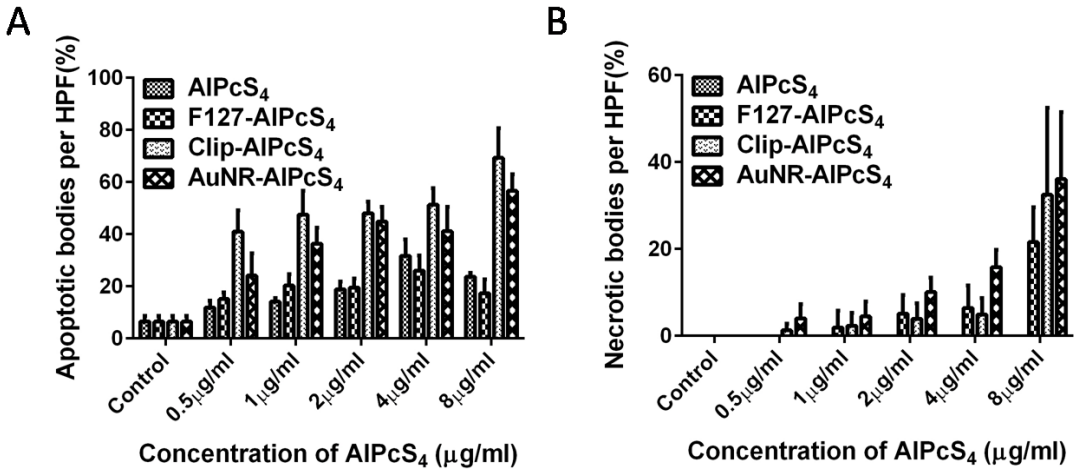

Figure S11: Apoptosis and necrosis quantized assay of $AlPcS_4$, F127-$AlPcS_4$, Clip-$AlPcS_4$, and AuNR-$AlPcS_4$ in gastric cancer cells. Cell percentage with apoptotic (A) or necrotic characteristics (B) among 200 cells at high power field was counted. The data represent the average of the three experiments and the bar is SD.

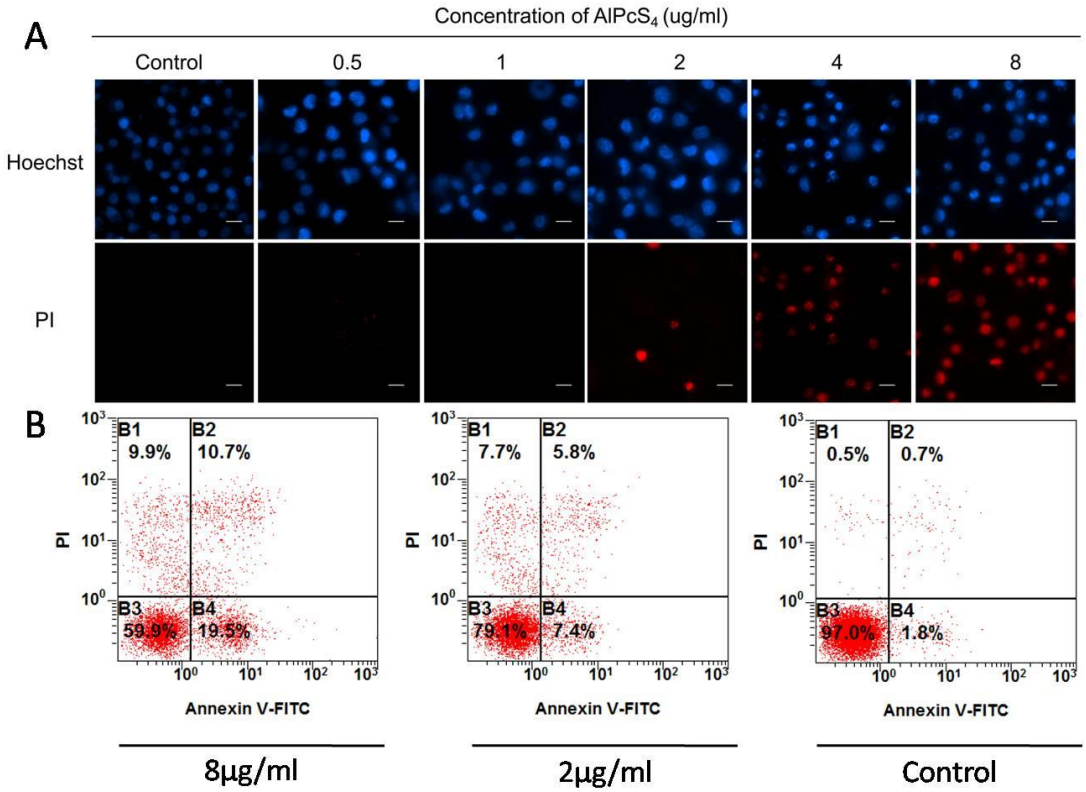

Figure S12: Apoptosis and necrosis induced by F127-$AlPcS_4$ carrier in SGC-7901 cells for 24hours (treatment time). SGC-7901 cells were treated with F127-$AlPcS_4$ at 0.5-8μg concentrations for 24hours, irradiated by 635nm laser light, incubated again for 24hours, and then stained with Hoechst and PI dyes for stain assay (A) or stained with Annexin V-FITC and PI dyes for Flow cytometry assay (B). Bar=20μm.